A generalized any-particle propagator theory: Prediction of proton affinities and acidity properties with the proton propagator

Cite as: J. Chem. Phys. **138**, 194108 (2013); https://doi.org/10.1063/1.4805030
Submitted: 22 January 2013 . Accepted: 25 April 2013 . Published Online: 21 May 2013

Manuel Díaz-Tinoco, Jonathan Romero, J. V. Ortiz, Andrés Reyes, and Roberto Flores-Moreno

A generalized any-particle propagator theory: Prediction of proton affinities and acidity properties with the proton propagator

Manuel Díaz-Tinoco,[1,2] Jonathan Romero,[3] J. V. Ortiz,[2] Andrés Reyes,[3,a)] and Roberto Flores-Moreno[1,b)]

[1]*Departamento de Química, Universidad de Guadalajara, Blvd. Marcelino García Barragán 1421, Guadalajara Jal., C. P. 44430, Mexico*
[2]*Department of Chemistry and Biochemistry, Auburn University, Auburn, Alabama 36849-5312, USA*
[3]*Department of Chemistry, Universidad Nacional de Colombia, Av. Cra. 30 #45-03 Bogotá, Colombia*

(Received 22 January 2013; accepted 25 April 2013; published online 21 May 2013)

We have recently extended the electron propagator theory to the treatment of any type of particle using an Any-Particle Molecular Orbital (APMO) wavefunction as reference state. This approach, called APMO/PT, has been implemented in the LOWDIN code to calculate correlated binding energies, for any type of particle in molecular systems. In this work, we present the application of the APMO/PT approach to study proton detachment processes. We employed this method to calculate proton binding energies and proton affinities for a set of inorganic and organic molecules. Our results reveal that the second-order proton propagator (APMO/PP2) quantitatively reproduces experimental trends with an average deviation of less than 0.41 eV. We also estimated proton affinities with an average deviation of 0.14 eV and the proton hydration free energy using APMO/PP2 with a resulting value of −270.2 kcal/mol, in agreement with other results reported in the literature. Results presented in this work suggest that the APMO/PP2 approach is a promising tool for studying proton acid/base properties. © *2013 AIP Publishing LLC*. [http://dx.doi.org/10.1063/1.4805030]

I. INTRODUCTION

Electronic structure methods based on electron propagator theory (EPT) are nowadays well established for the accurate computation of electron binding energies (EBEs) in molecular systems.[1–17] One of the most appealing features of the EPT is that only one calculation needs to be performed to obtain a detailed description of ionization phenomena of molecular systems. In addition, EPT calculations are more computationally efficient than other post-Hartree-Fock methods of comparable accuracy.

Recently, we developed a generalized Any-Particle Molecular Orbital Propagator method (APMO/PT) to study several quantum species using an Any-Particle Molecular Orbital Hartree-Fock (APMO/HF) wavefunction as a reference state.[18] This reference state has been previously employed to simultaneously study electronic and nuclear wavefunctions as well as systems comprising exotic particles[19–31] and propagators methods has been applied to study positronic–electronic systems.[32] Recently, the APMO/PT approach has been employed to study hydrogen nuclear quantum effects (NQEs) on the electronic ionization energies of prototypical molecular systems.[18]

A natural next step along the lines of this research is to explore the applicability of the generalized propagator method to study detachment processes of other particles such as protons. To that aim in this work we calculate proton binding energies (PBEs), proton affinities (PAs), and proton solvation energies. An accurate and efficient determination of these quantities is of utmost importance in studies concerning molecular processes such as acid-base and tautomeric rearrangement reactions, proton transfer, and hydrogen bonding phenomena.

An outline of this paper is as follows: In Sec. II we summarize the APMO/HF approach and the second-order proton propagator theory (APMO/PP2). In Sec. III we provide information on how the calculations are performed. In Sec. IV we report APMO/HF and APMO/PP2 calculations of PBEs, PAs, the proton hydration free energy and comparisons with experimental data. In Sec. V we summarize and provide concluding remarks.

II. THEORY

In this section we summarize the generalized any particle propagator theory[18] and explain how it is employed to calculate proton binding energies of molecular systems.

A. APMO/HF theory

The molecular Hamiltonian, H^{TOT}, includes contributions from N^Q quantum species ($\alpha, \beta, \gamma, \ldots$) and classical particles (N^C), such that

$$H^{TOT} = \sum_{\alpha}^{N^Q}\Bigg[-\sum_{i}^{N^\alpha}\frac{1}{2M_i}\nabla_i^2 + \sum_{i}^{N^\alpha}\sum_{j>i}^{N^\alpha}\frac{Q_\alpha^2}{r_{ij}} + \sum_{i}^{N^\alpha}\sum_{p}^{N^C}\frac{Q_\alpha Q_p}{r_{ip}} + \sum_{\beta>\alpha}^{N^Q}\sum_{i}^{N^\alpha}\sum_{I}^{N^\beta}\frac{Q_\alpha Q_\beta}{r_{iI}}\Bigg] + \sum_{p}^{N^C}\sum_{q>p}^{N^C}\frac{Q_p Q_q}{r_{pq}}, \quad (1)$$

a)Electronic mail: areyesv@unal.edu.co
b)Electronic mail: roberto.floresm@red.cucei.udg.mx

where i (I, ...) stands for the particle index of species α (β, ...), Q_α (Q_β, ...) is the charge of a particle of the type α (β, ...), N^α (N^β, ...) is the number of particles belonging to species α (β, ...) and Q_p is the charge of a classical particle. At the APMO/HF level, the molecular wavefunction, Ψ_0, is approximated as a product of single-configurational wavefunctions, Φ^α, for different types of quantum species:

$$\Psi_0 = \prod_{\alpha}^{N^Q} \Phi^\alpha. \tag{2}$$

Each Φ^α is represented in terms of molecular orbitals (MO), ψ_i^α. These ψ_i^α are obtained by solving the equations

$$f^\alpha(i)\psi_i^\alpha = \varepsilon_i^\alpha \psi_i^\alpha, \quad \forall i, \alpha. \tag{3}$$

Each f^α(i) is an effective one-particle Fock operator for quantum species α written as

$$f^\alpha(i) = h^\alpha(i) + {Q_\alpha}^2 \sum_{j}^{N^\alpha} \left[J_j^\alpha \mp K_j^\alpha \right] + Q_\alpha \sum_{\beta\neq\alpha}^{N^Q} \sum_{I}^{N^\beta} Q_\beta J_I^\beta. \tag{4}$$

In the above equation $h^\alpha(i)$ is the one-particle core Hamiltonian,

$$h^\alpha(i) = -\frac{\nabla_i^2}{2M_\alpha} + \sum_{p}^{N^C} \frac{Q_p Q_\alpha}{r_{ip}} \tag{5}$$

and J^α and K^α are Coulomb and exchange operators defined as

$$J_j^\alpha(1)\psi_i^\alpha(1) = \left[\int d\mathbf{r}_2 \psi_j^{\alpha *}(2) \frac{1}{r_{12}} \psi_j^\alpha(2) \right] \psi_i^\alpha(1), \tag{6}$$

$$K_j^\alpha(1)\psi_i^\alpha(1) = \left[\int d\mathbf{r}_2 \psi_j^{\alpha *}(2) \frac{1}{r_{12}} \psi_i^\alpha(2) \right] \psi_j^\alpha(1). \tag{7}$$

The sign preceding the exchange operator in Eq. (4) is chosen depending on the bosonic (positive) or fermionic (negative) nature of the α particles. In previous studies it has been observed that the exchange integrals between individual nuclei are always negligible and as a result they are neglected in our numerical treatment.[18,22]

B. APMO propagator theory

Here we summarize the derivation of the APMO propagator theory (APMO/PT). More details are found in Ref. 18. For a system comprising N^Q fermionic species {α, β,...} the spectral representation of a pq element of one-α-particle Green function is given by

$$G_{pq}^\alpha(\omega^\alpha) = \sum_m \frac{\langle \Psi(N^\alpha, N^\beta, \ldots) | a_p | \Psi^m(N^\alpha + 1, N^\beta, \ldots) \rangle \langle \Psi^m(N^\alpha + 1, N^\beta, \ldots) | a_q^\dagger | \Psi(N_\alpha, N_\beta, \ldots) \rangle}{\omega^\alpha - E_m(N_\alpha + 1, N_\beta, \ldots) + E_0(N_\alpha, N_\beta, \ldots)}$$
$$+ \sum_n \frac{\langle \Psi(N^\alpha, N^\beta, \ldots) | a_q^\dagger | \Psi^n(N^\alpha - 1, N^\beta, \ldots) \rangle \langle \Psi^n(N^\alpha - 1, N^\beta, \ldots) | a_p | \Psi(N_\alpha, N_\beta, \ldots) \rangle}{\omega^\alpha - E_n(N_\alpha - 1, N_\beta, \ldots) + E_0(N_\alpha, N_\beta, \ldots)}. \tag{8}$$

Here $|\Psi^n(N^\alpha - 1, N^\beta, \ldots)\rangle$ ($|\Psi^n\rangle$ in the rest of the text) stands for the exact wavefunction for a state n containing $N_\alpha - 1$, N_β, ... particles of each species and $E_n(N_\alpha - 1, N^\beta, \ldots)$ is its corresponding energy. On the other hand $|\Psi^m(N^\alpha + 1, N^\beta, \ldots)\rangle$ ($|\Psi^m\rangle$ in the rest of the text) stands for the exact wavefunction for a state m containing $N_\alpha + 1$, N_β, ... particles of each species and $E_m(N_\alpha + 1, N^\beta, \ldots)$ is its corresponding energy. The parameter ω^α has energy units. It can be inferred that the poles of Eq. (8) correspond to exact binding energies for particles of the species α.

If the APMO/HF reference state $|\Psi_0\rangle$ is employed, $|\Psi\rangle$ can be expanded as

$$|\Psi\rangle = \mathcal{N}^{-1/2} \Bigg\{ 1 + \sum_{\alpha}^{N^Q} \sum_{i,a\in\alpha} \kappa_i^a a_a^\dagger a_i + \sum_{\alpha}^{N^Q} \sum_{\beta>\alpha}^{N^Q} \sum_{\substack{i,a \\ I,A}} \kappa_{iI}^{aA} a_a^\dagger a_A^\dagger a_I a_i + \ldots \Bigg\} |\Psi_0\rangle, \tag{9}$$

where $\mathcal{N}$ is a normalization constant and $|\Psi_0\rangle$ is the APMO/HF wavefunction, as defined in Eq. (2); where i, j, ... (a, b, ...) stand for occupied (virtual) orbitals of α particles and I, J, ... (A, B, ...) stand for occupied (virtual) orbitals of β particles and so on. The correlation coefficients, κ, are obtained from Rayleigh–Schrödinger perturbation theory.[24,30,33,34] Following Pickup and Goscinski[3] now we introduce the superoperator metric, defined as

$$(A|B) = \langle \Psi | [A^\dagger, B]_+ | \Psi \rangle, \tag{10}$$

where A and B are two arbitrary operators (i.e., linear combinations of products of fermion-like creation or annihilation operators). The identity and Hamiltonian superoperators, $\hat{I}$ and $\hat{H}$, can be defined as

$$\hat{I} A = A, \tag{11}$$

$$\hat{H} A = [A, H^{TOT}]_- = A H^{TOT} - H^{TOT} A, \tag{12}$$

where the Hamiltonian, H^{TOT}, is the APMO Hamiltonian in its second quantized form:

$$H^{TOT} = \sum_{\alpha}^{N^{Q}} \left(H_0^{\alpha} + V_1^{\alpha} + V_2^{\alpha}\right) \tag{13}$$

with

$$H_0^{\alpha} = \sum_{p\in\alpha} (\lambda^{\alpha})^2 \varepsilon_p^{\alpha} a_p^{\dagger} a_p, \tag{14}$$

$$V_1^{\alpha} = \sum_{p,q,r,s\in\alpha} (\lambda^{\alpha})^2 \langle pq||rs\rangle \left[\frac{1}{4} a_p^{\dagger} a_q^{\dagger} a_s a_r - \delta_{qs}\langle n_q\rangle a_p^{\dagger} a_r\right], \tag{15}$$

$$V_2^{\alpha} = \sum_{\beta\neq\alpha}^{N^{Q}} \sum_{\substack{p,q\in\alpha \\ P,Q\in\beta}} \lambda^{\alpha}\lambda^{\beta} \langle pP|qQ\rangle \times \left[\frac{1}{2} a_p^{\dagger} a_P^{\dagger} a_Q a_q - \delta_{PQ}\langle n_P\rangle a_p^{\dagger} a_q\right]. \tag{16}$$

Here, ε_p^{α} is the pth orbital energy for species α and λ^{α} and λ^{β} include the effects of signs and charges of species α and β. Employing the above definitions, it is possible to express the α propagator matrix as

$$\mathbf{G}^{\alpha}(\omega^{\alpha}) = (\mathbf{a}^{\alpha}|(\omega^{\alpha}\hat{I} - \hat{H})^{-1}\mathbf{a}^{\alpha}), \tag{17}$$

where $\mathbf{a}^{\alpha}$ contains all the single annihilation operators, $\{a_i^{\alpha}, a_a^{\alpha}\}$.

By applying Löwdin's inner projection technique[35] with an appropriate superoperator space $\mathbf{h}^{\alpha}$,[18] the inversion of the super-operator resolvent in Eq. (17) is avoided and only one matrix inversion is needed,

$$\mathbf{G}^{\alpha}(\omega^{\alpha}) = (\mathbf{a}^{\alpha}|\mathbf{h}^{\alpha})(\mathbf{h}^{\alpha}|(\omega^{\alpha}\hat{I} - \hat{H})\mathbf{h}^{\alpha})^{-1}(\mathbf{h}^{\alpha}|\mathbf{a}^{\alpha}). \tag{18}$$

The super-operator space, $\mathbf{h}^{\alpha}$, is defined in such a way that it changes the number of α particles by one, while conserving the number of particles of the other species:

$$\begin{aligned}
\mathbf{h}^{\alpha} &= \{\mathbf{a}^{\alpha}\} \cup \left\{\mathbf{f}_{\mathbf{3}}^{\alpha}\right\} \cup \left\{\mathbf{f}_{\mathbf{5}}^{\alpha}\right\} \cup \ldots \\
\mathbf{h}^{\alpha} &= \{\mathbf{a}^{\alpha}\} \cup \left\{\mathbf{f}_{\mathbf{3}}^{\alpha\alpha\alpha}, \mathbf{f}_{\mathbf{3}}^{\beta\alpha\beta}, \mathbf{f}_{\mathbf{3}}^{\gamma\alpha\gamma} \ldots\right\} \cup \left\{\mathbf{f}_{\mathbf{5}}^{\alpha}\right\} \cup \ldots \\
\mathbf{h}^{\alpha} &= \{a_a, a_i\} \cup \{a_i^{\dagger} a_a a_b, a_a^{\dagger} a_i a_j, a_I^{\dagger} a_a a_A, a_A^{\dagger} a_i a_I, a_{\Gamma}^{\dagger} a_i a_{\Lambda}, \\
&\quad a_{\Lambda}^{\dagger} a_a a_{\Gamma}, \ldots\} \cup \left\{\mathbf{f}_{\mathbf{5}}^{\alpha}\right\} \cup \ldots.
\end{aligned} \tag{19}$$

The projection space, $\mathbf{h}^{\alpha}$, can be partitioned for convenience into primary, $\mathbf{a}^{\alpha\dagger} = \{a_a^{\alpha\dagger}, a_i^{\alpha\dagger}\}$ and complementary, $\mathbf{f}^{\alpha}$, spaces. The latter space contains operators associated to ionizations of an α particle coupled to excitations of any type of particle in the system. Using this partition, the propagator matrix can be rearranged and subsequently transformed into the expression

$$\mathbf{G}^{\alpha^{-1}}(\omega^{\alpha}) = (\mathbf{a}^{\alpha}|(\omega^{\alpha}\hat{I} - \hat{H})\mathbf{a}^{\alpha}) - (\mathbf{a}^{\alpha}|\hat{H}\mathbf{f}^{\alpha}) \times (\mathbf{f}^{\alpha}|(\omega^{\alpha}\hat{I} - \hat{H})\mathbf{f}^{\alpha})^{-1}(\mathbf{f}^{\alpha}|\hat{H}\mathbf{a}^{\alpha}), \tag{20}$$

which can also be presented as a Dyson-like equation[1]

$$\mathbf{G}^{\alpha^{-1}}(\omega^{\alpha}) = \mathbf{G}_{\mathbf{0}}^{\alpha^{-1}}(\omega^{\alpha}) - \Sigma^{\alpha}(\omega^{\alpha}) \tag{21}$$

with

$$\mathbf{G}_{\mathbf{0}}^{\alpha}(\omega^{\alpha})_{pq} = \frac{\delta_{pq}}{\omega^{\alpha} - \epsilon_p^{\alpha}}. \tag{22}$$

The self-energy matrix for the α-type particle, $\Sigma^{\alpha}(\omega^{\alpha})$, is defined by Eq. (21). Note that if an untruncated manifold is included in $\mathbf{f}^{\alpha}$, the poles of the propagator correspond to the exact one-particle binding energies. In order to arrive at a definite approximation for the self-energy, the perturbative expansion (Eq. (9)) and the operator space (Eq. (19)) must be truncated. The one α particle propagators at second and third order can be obtained by truncating $\mathbf{f}^{\alpha}$ to $\mathbf{f}_{\mathbf{3}}^{\alpha}$ (Eq. (19)).

A commonly used approximation neglects the off-diagonal elements of the self-energy matrix.[1] This is known as the diagonal approximation,

$$\omega_p^{\alpha} = \varepsilon_p^{\alpha} + \Sigma_{pp}^{\alpha}(\omega_p^{\alpha}), \tag{23}$$

where ε_p^{α} is the pth canonical orbital energy for the species α. Relaxation and correlation corrections to Koopmans' theorem results, ε_p^{α}, reside in the energy dependent self-energy term $\Sigma_{pp}^{\alpha(2)}(\omega_p^{\alpha})$. The latter term can be decomposed into intraspecies and interspecies contributions:

$$\Sigma_{pp}^{\alpha}(\omega^{\alpha}) = \Sigma_{pp}^{\alpha,\alpha}(\omega^{\alpha}) + \sum_{\beta\neq\alpha}^{N^{Q}} \Sigma_{pp}^{\alpha,\beta}(\omega^{\alpha}). \tag{24}$$

Although the diagonal approximation usually works well in the electronic structure applications of electron propagator theory, it is not clear yet if it will work well for the proton propagator.

C. Second-order quasiparticle self-energy for protons

In a system comprised quantum protons and electrons, corresponding to α and β types, respectively, the second order self-energy terms for a protonic orbital P, takes the following forms:

$$\Sigma_{PP}^{\alpha,\alpha(2)}(\omega_P) = \sum_{A,I>J\in\alpha} \frac{|\langle PA||IJ\rangle|^2}{\omega_P + \epsilon_A - \epsilon_I - \epsilon_J} + \sum_{I,A>B\in\alpha} \frac{|\langle PI||AB\rangle|^2}{\omega_P + \epsilon_I - \epsilon_A - \epsilon_B}, \tag{25}$$

$$\Sigma_{PP}^{\alpha,\beta(2)}(\omega_P) = \sum_{I\in\alpha} \sum_{a,i\in\beta} \frac{|\langle Pa|Ii\rangle|^2}{\omega_P + \epsilon_a - \epsilon_I - \epsilon_i} + \sum_{A\in\alpha} \sum_{i,a\in\beta} \frac{|\langle Pi|Aa\rangle|^2}{\omega_P + \epsilon_i - \epsilon_A - \epsilon_a}, \tag{26}$$

where $I, J, \ldots$ $(A, B, \ldots)$ stand for occupied (virtual) orbitals of protons (α) and $i, j, \ldots$ $(a, b, \ldots)$ stand for occupied (virtual) orbitals of electrons (β). Equations (25) and (26) are the working expressions for the calculation of PBEs, as corrections to the Koopmans-like results.

III. COMPUTATIONAL DETAILS

PBE calculations were performed with the APMO/PP2 method recently implemented in the LOWDIN software

package.[18,36] Atomic four-index integrals were calculated using the LIBINT package.[37] A modified version of the four-index transformation scheme proposed by Yamamoto and Nagashima[38] was employed to transform four-index integrals from the atomic to the molecular orbital basis. In all APMO/PP2 calculations, all hydrogen nuclei were treated quantum mechanically, while other nuclei were treated as classical particles. In these calculations the nuclear basis set centers were chosen to coincide with those of hydrogen nuclei in previous electronic structure optimization calculations.

In Subsection IV A, we compare experimental and theoretical APMO/HF and APMO/PP2 values of PBEs. APMO/HF and APMO/PP2 calculations were performed at the experimental geometries[39] with the aug-cc-pVTZ[40] electronic and $7s7p$[21] nuclear basis sets using the LOWDIN program.

In Subsection IV B, we report calculated PBEs for a set of organic molecules and compare them with reported PAs. The PA of molecule A was calculated by optimizing the molecular structure with an extra hydrogen atom, HA^+, employing the VWN[41] functional and the 6-311++G(2d,2p)[42–45] electronic basis set and the GEN-A2*[46,47] auxiliary basis set. Optimizations were performed using the deMon2k[48] software package. APMO/PP2 calculations were performed with the 6-311G[42,43] electronic and DZSPDN[23] nuclear basis sets using the LOWDIN program. The lowest PBE value for each molecule was reported and compared with the experimental PA.

In Subsection IV C, we study the solvation of a proton in water. Structures of the type $(H_2O)_nH^+$, with $n = 1$–7 were modeled. A stochastic algorithm was employed to explore the potential energy surface of these clusters and generate several cluster candidate structures. Candidate structures underwent further optimization with the PW91[49] density functional employing the 6-31++G**[50,51] orbital basis set and the GEN-A2*[46,47] auxiliary basis set, using the deMon2k[48] software.

In Subsection IV D, we estimate the proton hydration free energy. Total energies and PBEs of $(H_2O)_nH^+$ were calculated with APMO/HF and APMO/PP2 methods, respectively, employing 6-311G[42,43] electronic and DZSPDN nuclear basis set,[23] using the LOWDIN program.[36] After choosing the lowest PBE for each structure, the solvation energy of the proton was calculated as a Boltzmann average of all isomeric structures.[52,53]

IV. RESULTS FOR PROTON PROPAGATOR CALCULATIONS

A. Calculation of proton binding energies

We calculated the PBEs for a set of small A-X (X = H, D) molecules at the APMO/HF and APMO/PP2 levels of theory and compared them with experimental values determined via Threshold Ion-Pair Production Spectroscopy (TIPPS).[54–59] Results summarized in Table I reveal that propagator corrections are very large. For instance, we observe average deviations of 8.10 and 0.42 eV at the APMO/HF and APMO/PP2 levels, respectively. To reveal the nature of this correction, we decomposed the self-energy term (Eq. (24)) into pair-removal correlation (PRM), pair-relaxation (PRX), and orbital relaxation (ORX), by following the procedure proposed by Pickup and Goscinski.[3,60] For the inter-particle term we have

$$\begin{aligned}\Sigma_{pp}^{p+,e-(2)}(\omega_P) &= \mathrm{PRM} + \mathrm{PRX} + \mathrm{ORX} \\ &= \sum_A \sum_{i,a} \frac{|\langle Pi|Aa\rangle|^2}{\omega_P + \epsilon_i - \epsilon_A - \epsilon_a} \\ &\quad + \sum_{I\neq P} \sum_{a,i} \frac{|\langle Pa|Ii\rangle|^2}{\omega_P + \epsilon_a - \epsilon_I - \epsilon_i} \\ &\quad + \sum_{a,i} \frac{|\langle Pa|Pi\rangle|^2}{\omega_P + \epsilon_a - \epsilon_P - \epsilon_i}. \end{aligned} \tag{27}$$

The PRM and PRX terms are related to proton-electron correlation, while the ORX term is related to electron relaxation after proton release. For all the A-X systems considered in Table I, the PRX term becomes zero because there is only one occupied proton orbital and the intraspecies terms are zero because there is only one hydrogen nucleus present in each molecule.

For each of the molecular systems presented in Table I the magnitude of the ORX term is at least 50 times that of the PRM term. These results allow us to conclude that properly accounting for the relaxation of the electronic density is

TABLE I. Comparison between experimental and predicted PBEs calculated with APMO/HF and APMO/PP2 methods and decomposition analysis for $\Sigma_{PP}^{\alpha,\beta(2)}(\omega_P^\alpha)$ (in eV) for a set of small molecules. Electronic aug-cc-pVTZ[40] and protonic $7s7p$[21] basis sets were used.

			ΔSCF			$\Sigma_{PP}^{p^+,e^-(2)}$		
Molecule	Expt.[a]	KT[c]	Value	RXL	PP2[b]	PRM	ORX	Total
DF	16.1347	23.3426	15.8203	−7.5223	15.8705	0.1004	−7.5725	−7.4721
HF	16.0630	22.7339	15.5148	−7.2191	15.6708	0.1529	−7.2161	−7.0632
HCN	15.1563	23.6996	14.2678	−9.4318	14.8340	0.1566	−9.0222	−8.8656
DCl	14.4729	23.8216	13.7753	−10.0463	13.9819	0.0950	−9.9347	−9.8397
HCl	14.4178	23.1572	13.4825	−9.6747	13.7764	0.1488	−9.5295	−9.3808
$\lvert\boldsymbol{\Delta}\rvert$[d]		8.1020	0.6768		0.4222			

[a]Determined by TIPPS technique (Refs. 58, 59, and 62).
[b]APMO/PP2 calculations.
[c]Koopmans (APMO/HF) values.
[d]$|\boldsymbol{\Delta}|$: Average deviation from experiment.

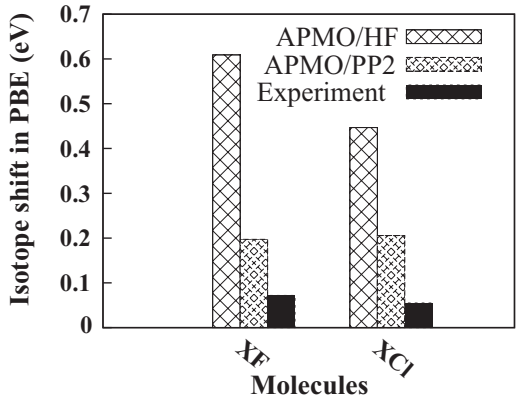

FIG. 1. Comparison between experimental and predicted isotope shifts in PBEs for HCl and HF molecules (in eV), employing APMO/HF and APMO/PP2 methods. Electronic aug-cc-pVTZ and protonic DZSPDN basis sets were used.

crucial for determining accurate PBEs. APMO/HF approach does not offer a quantitative description of the proton removal because Koopmans' approximation lacks relaxation effects. On the other hand, the APMO/PP2 approach recovers enough relaxation to provide an improved estimation of PBEs. This analysis shows that the proton ionization process keeps some characteristics of the ionization of internal electrons, where it is well known that relaxation effects are predominant.

Table I also includes PBEs calculated by the ΔSCF procedure[61] to estimate the relaxation effects at the APMO/HF level (RXL). Comparison of the ORX and RXL terms reveals that their magnitudes are similar, suggesting that most of the relaxation effects come from relaxation at the APMO/HF level.[1,3]

Another key feature of the APMO propagator theory is that it takes into account the mass effects of nuclei, thereby allowing the calculation of isotope effects on PBEs. Experimental data presented in Table I reveal that deuterated molecules present larger PBEs than their protonated counterparts. Figure 1 compares the magnitudes of the isotopic shifts on PBEs for HF and HCl molecules as calculated by APMO/HF and APMO/PP2 approaches. It shows that the APMO/PP2 approach provides better predictions of isotope shifts than the APMO/HF approach, although isotope shifts are still overestimated by a factor of 2-3.

B. Prediction of proton affinities

The proton affinity (PA) of a species A is an intrinsic acidity measure. It is defined as the negative of the enthalpy change of the gas-phase reaction:[63]

$$\mathrm{A} + \mathrm{H}^+ \rightarrow \mathrm{AH}^+ \quad PA(A) = -\Delta H = -\Delta E(T) + RT. \tag{28}$$

Here R is the universal gas constant, T is the absolute temperature, and ΔE is the energy difference between the AH^+ and the molecule A. In the case of a nonlinear polyatomic molecules, ΔE can be approximated as

$$\Delta E(T) = \Delta E_{rot}(T) + \Delta E_{trans}(T) + \Delta E_{vib}(T) + \Delta E_{ele}. \tag{29}$$

In an ideal gas approximation, $\Delta E_{trans}(T) = -\frac{3}{2}RT$, on the other hand $\Delta E_{rot}(T)$ becomes negligible due to[64] $\Delta E_{rot,AH^+}(T) \approx \Delta E_{rot,A}(T)$ and $\Delta E_{rot,H^+}(T) = 0$. After these considerations, the PA expression becomes

$$\mathrm{PA} = -\Delta E_{ele} - \Delta E_{vib} + \frac{5}{2}RT. \tag{30}$$

In APMO proton propagator calculations, PBEs account for changes due to proton release. In our calculations electrons and hydrogen nuclei are treated quantum mechanically, consequently, PBEs include ΔE_{ele} and part of ΔE_{vib}[65] (relaxation of quantum hydrogen atoms). The contributions to $\Delta E_{vib}(T)$ associated to the motion of classical nuclei is assumed to be close to zero, i.e., $\Delta E_{vib,A}(T) \approx \Delta E_{vib,HA^+}(T)$. Proton affinities for standard conditions of temperature and pressure (298.15 K and 1 bar) are approximated as

$$\mathrm{PA} \approx \mathrm{PBE(AH^+)} + 0.064\ \mathrm{eV}, \tag{31}$$

where $PBE(AH^+)$ is the proton binding energy of the species AH^+.

In Table II we contrast the calculated PAs using APMO methods (employing Eq. (31)) and experimental values[66–70] for a set of inorganic and organic molecules. The reported PAs are associated to the proton with the lowest PBE, highlighted with green circles in Figures 2–5. We observe in Table II that the total average deviation from experiment for APMO/PP2 is 0.14 eV (3.23 kcal/mol), which is one order of magnitude smaller than the average deviation with the APMO/HF method. Table II also shows partial average deviations calculated for molecules with the same functional group. We observe that predictions with the APMO/PP2 method for amines and carboxylic acids are in excellent agreement with experiment, with average deviations of 0.02 (0.46) and 0.12 (2.77) eV (kcal/mol). Figures 2 and 3 compare observed experimental trends for PAs associated to the homologous series of amines and carboxylic acids with those calculated with APMO methods. We observe that both APMO/HF and APMO/PP2 reproduce the decreasing trend in the acidity of the ammonium ions (associated to to the increasing trend in

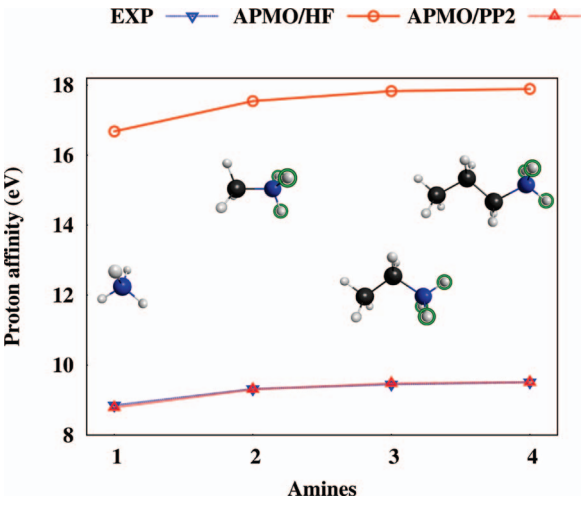

FIG. 2. Proton affinities for primary amines (in kcal/mol), calculated at APMO/HF and APMO/PP2 levels. Electronic 6-311G and protonic DZSPDN basis sets were used.

TABLE II. Comparison between experimental and predicted proton affinities (in eV) using APMO/HF and APMO/PP2 methods (Eq. (31)) for a set of organic and inorganic molecules. Electronic 6-311G and protonic DZSPDN basis sets were employed.[a]

Molecule	Proton affinity		
	Expt.[b]	KT[c]	P2[d]
Amines			
NH_3	8.85	16.68	8.79
CH_3NH_2	9.32	17. 54	9.31
$CH_3CH_2NH_2$	9.45	17.83	9.48
$CH_3CH_2CH_2NH_2$	9.51	17.89	9.51
$(CH_3)_2NH$	9.63	18.21	9.64
$(CH_3)_3N$	9.84	18.68	9.82
$\|\Delta\|$[e]		8.37	0.02
Aromatic			
$C_6H_5NH_2$	9.15	17.78	9.31
$C_6H_5COO^-$	14.75	22.97	15.07
$C_6H_5O^-$	15.24	23.70	15.53
$\|\Delta\|$[e]		8.44	0.26
Inorganic			
HS^-	15.31	24.24	14.82
CN^-	15.31	23.60	14.80
NO_2^-	14.75	22.72	14.77
$\|\Delta\|$[e]		8.40	0.34
Carboxylic acids			
$HCOO^-$	14.97	22.66	14.86
CH_3COO^-	15.11	23.04	15.22
$CH_3CH_2COO^-$	15.07	23.04	15.17
$CH_3(CH_2)_2COO^-$	15.03	23.09	15.23
$CH_3(CH_2)_3COO^-$	15.01	23.09	15.24
CH_2FCOO^-	14.71	22.41	14.65
CHF_2COO^-	14.32	21.92	14.19
CF_3COO^-	13.99	21.54	13.85
$ClCH_2COO^-$	14.58	22.43	14.63
$Cl(CH_2)_2COO^-$	14.78	22.53	14.68
CH_3COCOO^-	14.46	22.40	14.60
$\|\Delta\|$[e]		7.83	0.12
$\|\Delta\|$[e] Total		8.12	0.14

[a]Geometries optimized at VWN/6-311++G(2d,2p) level. Regular electronic structure calculation.
[b]References 66–70.
[c]APMO/HF proton affinities.
[d]APMO/PP2 proton affinities.
[e]$|\Delta|$: Average absolute difference.

basicity of amines) and the decreasing trend in the acidity of carboxylic acids. However, only APMO/PP2 produces quantitatively accurate results.

For aromatic and inorganic molecules we observe larger deviations. This can be attributed to large nuclear relaxation effects that are not completely recovered at the APMO/PP2 level. Therefore, higher order proton propagators are required for more accurate calculations of the PAs of these systems. Work is in progress in our laboratories to implement third order methods.

Despite the observed limitations, APMO/PP2 calculations are capable of providing reliable predictions of PAs, reproducing chemical trends in acidity. For instance, in Figures 4 and 5 we present calculated PAs for series of substituted organic compounds. We observe in Figure 4 how

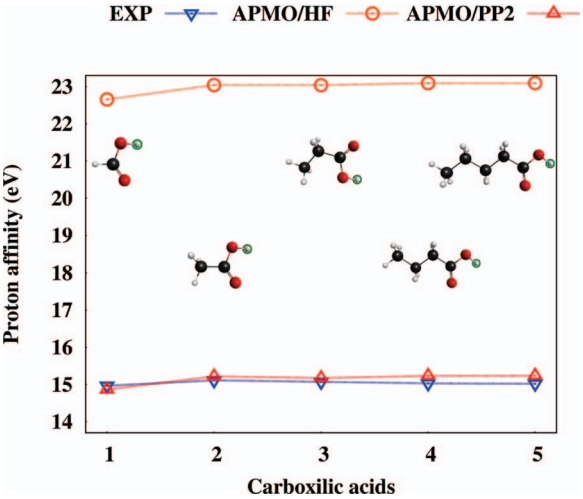

FIG. 3. Proton affinities for terminal carboxylic acids (in kcal/mol), calculated at APMO/HF and APMO/PP2 level. Electronic 6-311G and protonic DZSPDN basis sets were used.

APMO/PP2 calculations properly predict differences in acidity between primary, secondary, and ternary amine ions. Inductive effects in acetic acid are also well described, as shown in Figure 5.

C. Analysis of protonated water structure employing PBEs

A PBE, when defined as a measure of the energy required to extract a selected proton from a molecule, can be employed to analyze the propensity of a proton to be released. This feature is exploited here to study of proton hydration.

To that aim, we calculated total energies and PBEs for a set of protonated water clusters, $(H_2O)_nH^+$, employing the APMO/HF and APMO/PP2 approaches. Geometries for clusters containing $n = 2$–7 water molecules were generated by employing a stochastic search algorithm. A total of 10, 20,

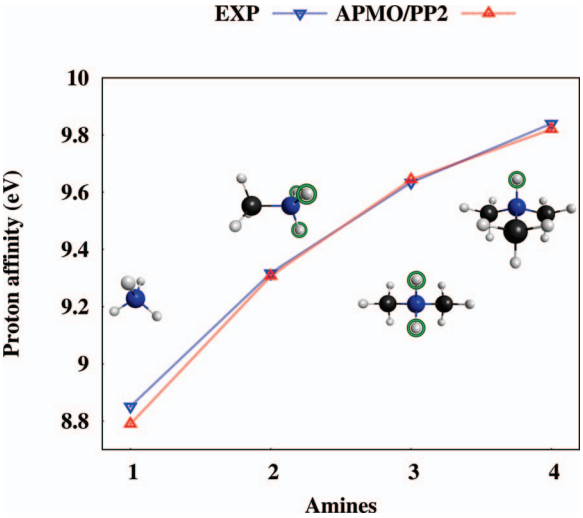

FIG. 4. Proton affinities for substituted amines (in kcal/mol), calculated at APMO/PP2 level. Electronic 6-311G and protonic DZSPDN basis sets were used.

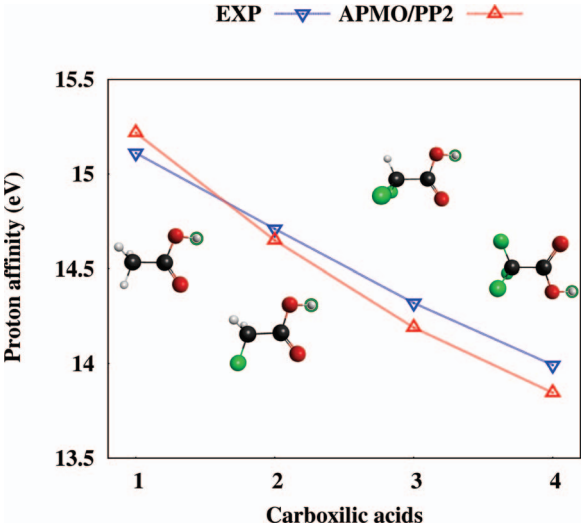

FIG. 5. Proton affinities for substituted cloro-acetic acids (in kcal/mol), calculated at APMO/PP2 level. Electronic 6-311G and protonic DZSPDN basis sets were used.

11, 26, 16, and 18 structures were generated for $n = 2$–7, respectively. Additional geometries, reported by Hodges and Stone[71] were also considered in this analysis. Details are given in Sec. III.

Of all possible geometries generated for each n, we analyzed only those presenting the Lowest Total Energy (LTE) and the Lowest Proton Binding Energy (LPBE). LTE structures are of special importance because they are expected to resemble the most stable geometrical configuration of a hydrated proton in solution whereas LPBE structures are related to geometrical configurations where protons can be more easily donated. The geometries of LTE and LPBE are shown in Table III.

We observe that the LTE and LPBE structures for $n = 1$ are the same. Structures for $n = 2$, 3 are very similar, presenting only small variations in dihedral angles between water molecules. For $n = 4$ the LTE structure is the $H_9O_4^+$ eigencation, where the H_3O^+ cation is linked to three water molecules through single hydrogen bonds. This structure has been already identified as the most likely solvation structure for the hydrated proton.[72] In contrast, the LPBE structure presents a four-member ring comprising an H_3O^+ cation and three water molecules, one of them linked to the other two through a two-donor one acceptor hydrogen bond. Similar ring configurations have been observed in pure water clusters.[73–75]

At this stage large differences in the distribution of PBEs are observed. As shown in Table IV, for structures with $n = 4$, differences in PBEs between all the protons of the LTE structures do not exceed 1.2 kcal/mol. These results indicate that in the case of the $H_9O_4^+$ eigencation, protons are already equivalent. This effect can be associated to "proton resonances" observed in molecular dynamics simulations.[72] In contrast, differences in the PBEs for the LPBE structures reach up to 16.4 kcal/mol and protons are consequently not equivalent. Protons associated to the double acceptor water molecule present the smallest PBEs for $n \geq 4$, as shown in Table III. This finding indicates that proton detachment on

TABLE III. Protonated water clusters with the Lowest Total Energy (LTE) and the Lowest Proton Binding Energy (LPBE) for $n = 1$–7. Protons with the lowest PBEs are highlighted with green circles.

n[a]	LTE[b]	LPBE[c]
1	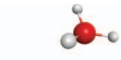	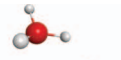
2	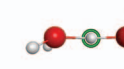	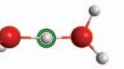
3	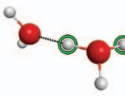	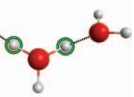
4	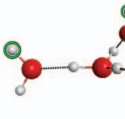	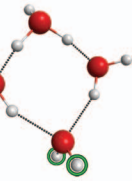
5	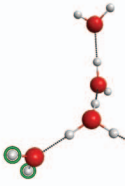	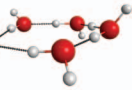
6	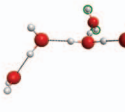	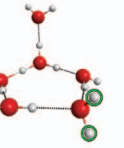
7	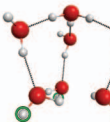	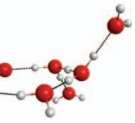

[a]Number of water molecules.
[b]Structure with the lowest total energy.
[c]Structure with the lowest proton binding energy.

the LPBE structure produces a hydroxyl anion, that eventually leads to a ring structure where a H_3O^+ and OH^- coexist.

For $n > 4$, LTE structures present a $H_9O_4^+$ eigencation surrounded by water molecules forming single hydrogen bonds. For $n = 7$, protons in the water molecules attached to the $H_9O_4^+$ cation have the smallest PBEs and are expected to be more reactive. For $n > 4$, LPBE structures maintain the features of the LPBE with $n = 4$, exhibiting ring structures composed by a H_3O^+ cation and water molecules. As for $n = 4$, the ring comprises a double hydrogen-bond acceptor water molecule that has the protons with the smallest PBE.

Table IV also shows differences in total energies (DTE) and differences in lowest PBEs (DPBE) between LTE and LPBE structures, revealing that DTE are always smaller than DPBE for $n > 2$. This fact suggests that although LTE and LPBE structures have similar total energies and can coexist in gas phase and even in liquid water, the LPBE configurations are considerably more reactive towards proton transfer than LTE structures.

In summary, the study of PBEs and total energies of protonated water clusters allows us to conclude that protons with the largest susceptibility to be released, present in LPBE

TABLE IV. Lowest and highest proton binding energies (PBEs) calculated for protonated water clusters with the Lowest Total Energy (LTE) and the Lowest Proton Binding Energy (LPBE) for $n = 1$–7. Differences in total energies and lowest PBEs between LTE and LPBE structures are also included. The APMO/PP2 method, with electronic 6-311G and protonic DZSPDN basis sets, was used. All values in kcal/mol.

	LTE[b]		LPBE[c]			
n[a]	LPBE[f]	HPBE[g]	LPBE[f]	HPBE[g]	DTE[d]	DPBE[e]
1	156.1	156.1	156.1	156.1	0.00	0.00
2	205.4	220.2	204.8	219.8	0.30	0.68
3	246.0	256.9	242.9	256.0	0.67	3.02
4	274.4	275.6	252.3	268.7	4.53	22.06
5	284.2	300.5	262.1	289.9	2.96	22.10
6	289.9	318.6	261.6	312.0	5.49	28.30
7	280.1	298.0	267.6	324.1	8.91	12.46

[a]Number of water molecules.
[b]Structure with the lowest total energy.
[c]Structure with the lowest proton binding energy.
[d]Difference in total energy between LTE and LPBE structures.
[e]Difference in lowest PBE between LTE and LPBE structures.
[f]Lowest proton binding energy in the structure.
[g]Highest proton binding energy in the structure.

structures, are not those belonging to H_3O^+ but those in double hydrogen-bond acceptor water molecules. We also point out that even when LTE and LPBE structures have similar total energies, they have different reactivities towards proton donation.

D. Estimation of proton hydration free energy

The proton hydration free energy, $\Delta G_{hyd}(H^+)$ is required for calculating acidity constants in water.[76–80] Regular approaches for estimating $\Delta G_{hyd}(H^+)$ usually involve taking the limit of the difference between free energies of neutral and protonated n-water clusters as n increases.[64,80,81]

Alternatively, we propose to utilize our propagator approach to estimate proton hydration energies by considering the PBEs calculated for the set of protonated water clusters of Sec. IV C. The proton hydration process can be associated to the following reaction:

$$H^+_{(gas)} \rightarrow H^+_{(aq)}. \tag{32}$$

As a first step, this process can be approximated by the reaction:

$$H^+_{(gas)} + (H_2O)_n \rightarrow H(H_2O)^+_n. \tag{33}$$

Enthalpies of Eq. (33) are calculated using Eqs. (28) and (31). The entropy change is obtained using this equation:

$$\Delta S = S_{H(H_2O)^+_n} - S_{(H_2O)_n} - S_{H^+_{(gas)}}, \tag{34}$$

where ΔS includes the entropy contribution of the free proton, $S(H^+)$, and the difference in entropy of the structures, $S_{H(H_2O)^+_n} - S_{(H_2O)_n}$. Calculation of the proton entropy change using the Sakur-Tetrode equation[64,76,82] yields the entropy factor, $T S_{H^+_{(gas)}} = 7.76$ kcal/mol at standard conditions of temperature and pressure (STD). Assuming that $S_{H(H_2O)^+_n} - S_{(H_2O)_n}$ is negligible, the change in entropy and the change in free energy can be approximated as

$$T\Delta S = -7.76 \text{ kcal/mol}, \tag{35}$$

$$\Delta G = \Delta H - T\Delta S, \tag{36}$$

$$\Delta G \approx \text{PBE} - \frac{5}{2}RT - (-7.76 \text{ kcal/mol}), \tag{37}$$

$$\Delta G \approx \text{PBE} + 6.28 \text{ kcal/mol}. \tag{38}$$

TABLE V. Thermodynamic properties: ΔE, ΔH, $T\Delta S$, and ΔG (in kcal/mol) calculated for protonated water clusters $n = 1$–7 employing the APMO/PP2 method. Electronic 6-311G and protonic DZSPDN basis sets were used.

n[a]	N[b]	PBE[c]	ΔE	ΔH	$T\Delta S$	ΔG
1	1	156.1	− 157.0	− 157.6	− 7.76	− 149.8
2	10	205.0	− 205.9	− 206.5	− 7.76	− 198.7
3	20	243.9	− 244.8	− 245.4	− 7.76	− 237.6
4	11	256.7	− 257.6	− 258.2	− 7.76	− 250.4
5	26	258.9	− 259.8	− 260.4	− 7.76	− 252.6
6	18	266.7	− 267.6	− 268.2	− 7.76	− 260.4
7	20	276.5	− 277.4	− 278.0	− 7.76	− 270.2

[a]Number of water molecules in cluster.
[b]Number of structures found.
[c]APMO/PP2 results.

Average ΔEs were calculated using Boltzmann factors that are based on the total energies of the cation and neutral clusters. The Boltzmann-weighted average energy of the cationic cluster is subtracted from its neutral counterpart to produce PBEs for a given n.

Thermodynamic properties calculated at the APMO/PP2 level using the previous equations are presented in Table V. Values of ΔG as a function of n are shown in Figure 6; results at APMO/HF level were also included for comparison.

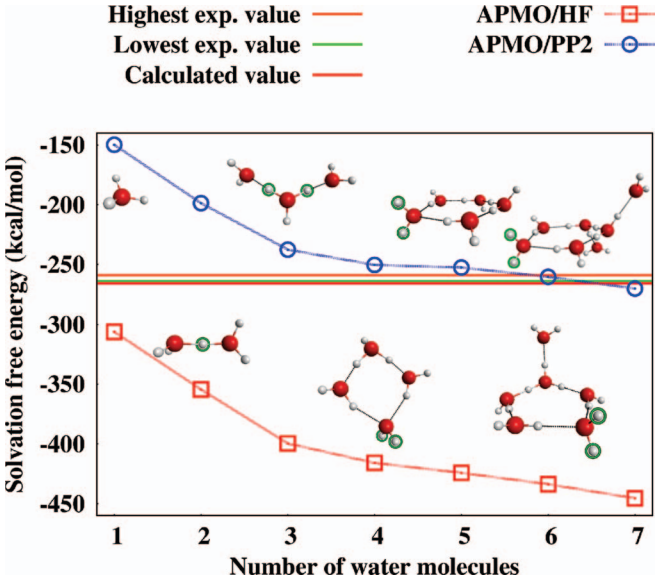

FIG. 6. Proton solvation energy free energies (in kcal/mol) calculated for protonated water clusters, ΔG, as a function of n, employing the APMO/PP2 method. Electronic 6-311G and protonic DZSPDN basis sets were used. Values quoted in literature[64,80,81,83,84] are included for comparison.

An analysis of our results reveals that trends in ΔG calculated at APMO/HF and APMO/PP2 level are similar, decreasing as n increases and presenting a smooth slope for $n > 3$. However, only the APMO/PP2 approach reproduces quantitatively proton hydration free energies, as evidenced by values of ΔG for $n = 6 - 7$ (-260.4 kcal/mol and -270.2 kcal/mol, respectively). These estimations are in excellent agreement with experimental and calculated proton hydration energies quoted in literature.[64,79–81,83,84]

We suggest that a faster convergence on ΔG with respect to n could be achieved by including long-range solvent effects, as shown by other authors.[64,80,81] Nevertheless, the results presented here demonstrate that the proton propagator is a promising tool for predicting acid/base properties such as the proton hydration free energy.

V. CONCLUSIONS

The recently proposed generalized any-particle propagator theory in its second order diagonal approximation has been utilized to calculate proton binding energies, proton affinities, and proton solvation energies. The results presented above show that electronic relaxation after proton detachment plays a central role in the energetics of the process. The results presented so far allow us to conclude that the proton propagator can be a useful tool for calculating and understanding acid/base chemistry. The accuracy of the APMO/PP2 method can be improved by including higher-order terms in the self-energy that are generated by improved any-particle reference states.[85,86] Future work will also be devoted to the estimation of pK_a values and the description of proton transfer processes.

ACKNOWLEDGMENTS

Funding for this work was provided by SEP-CONACyT (Basic Science Grant No. 127362), Universidad Nacional de Colombia (Grant No. QUIPU-201010016739), and the National Science Foundation (NSF) (Grant No. CHE–0809199 to Auburn University). The authors acknowledge Centro Universitario de los Lagos (CULAGOS) of the University of Guadalajara for computational resources and the support of Professor Francisco Tenorio Rangel and Professor Jaime Gustavo Rodríguez Zavala. We also thank Teresa Tamayo for helpful discussions. M.D.T. gratefully acknowledges a Master scholarship from CONACyT (257420).

[1] J. Linderberg and Y. Öhrn, *Propagators in Quantum Chemistry*, 2nd ed. (Wiley-Interscience, Hoboken, NJ, 2004).
[2] P. Jørgensen and J. Simons, *Second Quantization-Based Methods in Quantum Chemistry*, 1st ed. (Academic, New York, 1981).
[3] B. Pickup and O. Goscinski, Mol. Phys. **26**, 1013 (1973).
[4] Y. Öhrn and G. Born, *Advances in Quantum Chemistry* (Academic Press, 1981), Vol. 13, pp. 1–88.
[5] J. V. Ortiz, *Advances in Quantum Chemistry* (Academic Press, 1999), Vol. 35, pp. 33–52.
[6] L. S. Cederbaum and W. Domcke, Adv. Chem. Phys. **36**, 205 (1977).
[7] W. von Niessen, J. Schirmer, and L. Cederbaum, Comput. Phys. Rep. **1**, 57 (1984).
[8] J. Simons and W. D. Smith, J. Chem. Phys. **58**, 4899 (1973).
[9] M. F. Herman, K. F. Freed, and D. L. Yeager, *Analysis and Evaluation of Ionization Potentials, Electron Affinities, and Excitation Energies by the Equations of Motion–Green's Function Method*, Advances in Chemical Physics (Wiley, 1981), pp. 1–69.
[10] J. V. Ortiz, J. Chem. Phys. **104**, 7599 (1996).
[11] V. G. Zakrzewski, O. Dolgounitcheva, A. V. Zakjevskii, and J. V. Ortiz, Annu. Rep. Comput. Chem. **6**, 79 (2010).
[12] V. G. Zakrzewski, O. Dolgounitcheva, A. V. Zakjevskii, and J. V. Ortiz, Adv. Quantum Chem. **62**, 105 (2011).
[13] J. V. Ortiz, WIREs Comput. Mol. Sci. **3**, 123–142 (2013).
[14] R. Flores-Moreno, J. Melin, O. Dolgounitcheva, V. G. Zakrzewski, and J. V. Ortiz, Int. J. Quantum Chem. **110**, 706 (2010).
[15] L. S. Cederbaum, J. Phys. B. **8**, 290 (1975).
[16] L. S. Cederbaum, W. Domcke, J. Schirmer, and W. Von Niessen, Adv. Chem. Phys. **65**, 115 (1986).
[17] J. Schirmer, L. S. Cederbaum, and O. Walter, Phys. Rev. A **28**, 1237 (1983).
[18] J. Romero, E. Posada, R. Flores-Moreno, and A. Reyes, J. Chem. Phys. **137**, 074105 (2012).
[19] M. Tachikawa, K. Mori, H. Nakai, and K. Iguchi, Chem. Phys. Lett. **290**, 437 (1998).
[20] S. Webb, T. Iordanov, and S. Hammes-Schiffer, J. Chem. Phys. **117**, 4106 (2002).
[21] H. Nakai, Int. J. Quantum Chem. **86**, 511 (2002).
[22] H. Nakai and K. Sodeyama, J. Chem. Phys. **118**, 1119 (2003).
[23] A. Reyes, M. Pak, and S. Hammes-Schiffer, J. Chem. Phys. **123**, 064104 (2005).
[24] H. Nakai, Int. J. Quantum Chem. **107**, 2849 (2007).
[25] H. Nakai, Y. Ikabata, Y. Tsukamoto, Y. Imamura, K. Miyamoto, and M. Hoshino, Mol. Phys. **105**, 2649 (2007).
[26] P. Adamson, X. Duan, L. Burggraf, M. Pak, C. Swalina, and S. Hammes-Schiffer, J. Phys. Chem. A **112**, 1346 (2008).
[27] S. González, N. Aguirre, and A. Reyes, Int. J. Quantum Chem. **108**, 1742 (2008).
[28] T. Ishimoto, M. Tachikawa, and U. Nagashima, Int. J. Quantum Chem. **109**, 2677 (2009).
[29] T. Udagawa and M. Tachikawa, *Multi-Component Molecular Orbital Theory* (Nova Science Publishers, New York, 2009).
[30] S. González and A. Reyes, Int. J. Quantum Chem. **110**, 689 (2010).
[31] F. Moncada, D. Cruz, and A. Reyes, Chem. Phys. Lett. **539–540**, 209 (2012).
[32] M. Müller and L. S. Cederbaum, Phys. Rev. A **42**, 170 (1990).
[33] C. Møller and M. S. Plesset, Phys. Rev. **46**, 618 (1934).
[34] P.-O. Löwdin, J. Math. Phys. **6**, 1341 (1965).
[35] P.-O. Löwdin, Phys. Rev. **139**, A357 (1965).
[36] R. Flores-Moreno, S. A. González, N. F. Aguirre, E. F. Posada, J. Romero, F. S. Moncada, K. Pineda, M. Díaz, and A. Reyes, LOWDIN: A general code for the treatment of any quantum particle (2012), see https://sites.google.com/site/lowdinproject/home.
[37] J. T. Fermann and E. F. Valeev, LIBINT: Machine-generated library for efficient evaluation of molecular integrals over Gaussians (2003), see http://sourceforge.net/p/libint.
[38] S. Yamamoto and U. Nagashima, Comput. Phys. Commun. **166**, 58 (2005).
[39] *NIST Computational Chemistry Comparison and Benchmark Database, NIST Standard Reference Database Number 101, Release 15b, August 2011*, edited by R. D. Johnson III, *see* http://cccbdb.nist.gov.sci-hub.org/ *(Retrieved, November 24, 2011)*.
[40] T. Dunning, Jr., J. Chem. Phys. **90**, 1007 (1989).
[41] S. Vosko, L. Wilk, and M. Nusair, Can. J. Phys. **58**, 1200 (1980).
[42] A. McLean and G. Chandler, J. Chem. Phys. **72**, 5639 (1980).
[43] K. Raghavachari, J. Binkley, R. Seeger, and J. Pople, J. Chem. Phys. **72**, 650 (1980).
[44] T. Clark, J. Chandrasekhar, G. Spitznagel, and P. Schleyer, J. Comput. Chem. **4**, 294 (1983).
[45] M. Frisch, J. Pople, and J. Binkley, J. Chem. Phys. **80**, 3265 (1984).
[46] J. Andzelm, E. Radzio, and D. Salahub, J. Comput. Chem. **6**, 520 (1985).
[47] J. Andzelm, N. Russo, and D. Salahub, J. Chem. Phys. **87**, 6562 (1987).
[48] A. Köster, P. Geudtner, P. Calaminici, M. Casida, V. Dominguez, R. Flores-Moreno, G. Gamboa, A. Goursot, T. Heine, A. Ipatov *et al.*, deMon2k, Release 2.4.2, Cinvestav, Mexico-City, Mexico (2006), See http://www.demon-software.com.
[49] J. Perdew, P. Ziesche, and H. Eschrig, *Electronic Structure of Solids* (Academic-Verlag, Berlin, 1991).
[50] R. Ditchfield, W. Hehre, and J. Pople, J, Chem. Phys **54**, 724 (1971).
[51] W. Hehre, R. Ditchfield, and J. Pople, J. Chem. Phys. **56**, 2257 (1972).
[52] M. Saha, Phil. Mag. Ser. 6 **40**, 472 (2009).
[53] M. N. Saha, Philos. Mag. 6 **40**, 472 (1920).

[54]J. D. D. Martin, Ph.D. dissertation, University of Waterloo, 1998.
[55]J. Martin and J. Hepburn, J. Chem. Phys. **109**, 8139 (1998).
[56]R. Shiell, X. Hu, Q. Hu, and J. Hepburn, Faraday Discuss. **115**, 331 (2000).
[57]R. Shiell, X. Hu, Q. Hu, and J. Hepburn, J. Phys. Chem. A **104**, 4339 (2000).
[58]Q. Hu, T. Melville, and J. Hepburn, J. Chem. Phys. **119**, 8938 (2003).
[59]Q. Hu, Q. Zhang, and J. Hepburn, J. Chem. Phys. **124**, 074310 (2006).
[60]A. Szabo and N. S. Ostlund, *Modern Quantum Chemistry: Introduction to Advanced Electronic Structure Theory* (Dover Publications, New York, 1996).
[61]P. S. Bagus, Phys. Rev. **139**, A619 (1965).
[62]Q. Hu and J. Hepburn, J. Chem. Phys. **124**, 074311 (2006).
[63]A. McNaught and A. Wilkinson, *Compendium of Chemical Terminology* (Blackwell Science, Oxford, UK, 1997), Vol. 1669.
[64]G. Tawa, I. Topol, S. Burt, R. Caldwell, and A. Rashin, J. Chem. Phys. **109**, 4852 (1998).
[65]A. Bochevarov, E. Valeev, and C. Sherrill, Mol. Phys. **102**, 111 (2004).
[66]W. L. Jolly, *Modern Inorganic Chemistry*, 2nd ed. (McGraw-Hill, New York, 1991).
[67]E. Hunter and S. Lias, J. Phys. Chem. Ref. Data **27**, 413 (1998).
[68]J. Cumming and P. Kebarle, Can. J. Chem. **56**, 1 (1978).
[69]S. Graul, M. Schnute, and R. Squires, Int. J. Mass Spectrom. Ion Process. **96**, 181 (1990).
[70]K. Ervin, J. Ho, and W. Lineberger, J. Phys. Chem. **92**, 5405 (1988).
[71]M. Hodges and A. Stone, J. Chem. Phys. **110**, 6766 (1999).
[72]C. Knight and G. Voth, Acc. Chem. Res. **45**, 101 (2012).
[73]J. Pérez, C. Hadad, and A. Restrepo, Int. J. Quantum Chem. **108**, 1653 (2008).
[74]G. Hincapié, N. Acelas, M. Castao, J. David, and A. Restrepo, J. Phys. Chem. A **114**, 7809 (2010).
[75]F. Ramírez, C. Hadad, D. Guerra, J. David, and A. Restrepo, Chem. Phys. Lett. **507**, 229 (2011).
[76]K. Alongi and G. Shields, Annu. Rep. Comp. Chem. **6**, 113 (2010).
[77]M. Liptak and G. Shields, Int. J. Quantum Chem. **85**, 727 (2001).
[78]M. Liptak, K. Gross, P. Seybold, S. Feldgus, and G. Shields, J. Am. Chem. Soc. **124**, 6421 (2002).
[79]C. Kelly, C. Cramer, and D. Truhlar, J, Phys. Chem. A **110**, 2493 (2006).
[80]C. Kelly, C. Cramer, and D. Truhlar, J. Phys. Chem. B **110**, 16066 (2006).
[81]M. Tissandier, K. Cowen, W. Feng, E. Gundlach, M. Cohen, A. Earhart, J. Coe, and T. Tuttle, Jr., J. Phys. Chem. A **102**, 7787 (1998).
[82]D. McQuarrie, *Statistical Mechanics* (Harper & Row, New York, 1970).
[83]A. Rebollar-Zepeda, T. Campos-Hernández, M. Ramírez-Silva, A. Rojas-Hernández, and A. Galano, J. Chem. Theory Comput. **7**, 2528 (2011).
[84]J. Ho and M. Coote, J. Chem. Theory Comput. **5**, 295 (2009).
[85]M. Hoshino, H. Nishizawa, and H. Nakai, J. Chem. Phys. **135**, 024111 (2011).
[86]H. Nishizawa, Y. Imamura, Y. Ikabata, and H. Nakai, Chem. Phys. Lett. **533**, 100 (2012).